*35th EPS Conference on Plasma Phys. Hersonissos, 9 - 13 June 2008 ECA Vol.**32D**, P-4.099 (2008)*

Pellet Drift Modelling – Validation and ITER Predictions

F. Köchl[1], D. Frigione[2], L. Garzotti[3], G. Kamelander[1], H. Nehme[4], B. Pégourié[4], and JET EFDA contributors[*]

JET-EFDA, Culham Science Centre, OX14 3DB, Abingdon, UK

[1]Association EURATOM-ÖAW/ATI, Kegelgasse 27/3, 1030 Vienna, Austria

[2]Association EURATOM-ENEA, Frascati Research Centre, 00044 Frascati, Italy

[3]Association EURATOM-UKAEA Fusion, Culham Science Centre, OX14 3DB Abingdon, UK

[4]Association EURATOM CEA, CEA/DSM/DRFC, Centre de Cadarache, 13108 St-Paul-lez-Durance, France

1. Introduction

The pellet particle drift due to the gradient of the magnetic field has a strong influence on the plasma fuelling characteristics. It is directed towards the low field side of the torus and depends on various pellet and target plasma parameters. This phenomenon might play a vital role for the pellet fuelling capability in ITER. Therefore, many efforts are undertaken to analyse it in detail and to improve predictions. A first-principles code for the calculation of the pellet source profile, based on enhanced versions of an NGPS-type ablation [1] and a four fluids Lagrangian drift model [2], has recently been developed and benchmarked by comparison with drift measurements from the experiment and in full transport simulations. Methods and results are described in section 2. In section 3, scaling laws for the rough calculation of the drift displacement, based on a parameter scan performed with the pellet code, are presented. Section 4 deals with calculations of the drift behaviour in ITER.

2. Pellet Code Validation

In order to benchmark the pellet code, measurement data from pellet injections in FTU [3], Tore Supra [4], DIII-D [5], and JET [6] with different plasma conditions and pellet injection directions has been collected. The measured pellet drift, as obtained by evaluation of the barycentres for the pellet profiles before (ablation) and after the drift process (deposition), was compared with the simulation results. In the simulations, the exact plasma geometry was taken into account. The interaction of previously deposited pellet material on the ablation and drift of subsequent pellet material clouds (plasmoids), leading to pre-cooling effects, is considered by the code. The physical ablation process is treated in detail; in particular, a full Maxwellian description is used for incident electrons, and the impact of incident particles on the electrostatic sheath and partly ionised cloudlet zones is dealt with as carefully as possible [7]. In the drift model, the drift displacement is evaluated for each plasmoid at a number of points with varying distance to the plasmoid midpoint. The drift deceleration is determined by Alfvén wave propagation [8,9], as well as parallel resistive currents outside [2]

[*] *See the Appendix of M.L.Watkins et al., Fusion Energy 2006 (Proc. 21st Int. Conf. Chengdu, 2006) IAEA, (2006)*

and inside the plasmoid [9]. Benchmarking results for several tokamak scenarios are shown in Tab.1. With exception of the pellet injection in DIII-D, the predicted average particle displacement lies within the error range of the measurement, which is however usually in the order of the measurement quantity itself. The pellet code has also been tested in full transport simulations with JETTO. Simulations of the JET shot #49030 [10] were redone using the JETTO mixed Bohm/gyroBohm implementation. Results are shown in Fig.1-2. Since the pellets are not always fully ablated, the pellet pre-cooling effect can lead to increased particle loss and a decrease in fuelling efficiency, which is compensated by deeper penetration caused by the ∇B-drift. For this reason, the difference to the simulations done with the JETTO NGPS pellet module is rather small.

3. Scaling Law for ∇B-Drift

Based on a set of ~800 simulations with varying injection and plasma target parameters in the vicinity of typical tokamak configurations (~ ±40% of standard parameter settings), least square fits have been carried out to determine the main parameter dependencies and to derive an equation for the rough calculation of the absolute average particle drift displacement in terms of the flux coordinate $(R_{max} - R_{min})/2$:

$$\Delta_{\mathrm{Drift}} = C_1 \left(\frac{V_p}{100}\right)^{C_2} r_p^{C_3} n_{e0}^{C_4} T_{e0}^{C_5} \left(\left|\alpha\right| - C_6\right| + C_8\right)^{C_7} (1-\Lambda)^{C_9} a_0^{C_{10}} R_0^{C_{11}} B_0^{C_{12}} \kappa^{C_{13}},$$

with injection velocity V_p (m/s), pellet radius r_p (mm), axial density n_{e0} (10^{19} m^{-3}) and electron temperature T_{e0} (keV), injection angle $\alpha \in [-\pi,\pi]$, impact parameter of the pellet trajectory Λ (norm. minor radius), minor radius a_0 (m), major radius R_0 (m), toroidal field B_0 (T), and plasma elongation κ. To avoid statistical artefacts in the calculation coming from the rational q-surface effect on the drift damping behaviour [2,4], which itself cannot easily be described as part of a scaling fit formula, the q-profile was changed arbitrarily for each simulation run ($q_{edge} \in [3,9]$). Only pellets that are ablated before reaching the tangency point of the trajectory with the flux surfaces were considered. The results and rms errors obtained for the constants C_1-C_{13} for two different assumptions concerning the parameter space to be analysed are summarised in Tab.2. Constants for the determination of the ablation and deposition barycentres are also given. As expected, the drift displacement is strongly correlated to the pellet size and injection velocity, as well as to the magnetic field strength. Due to correlation effects, some parameters like Λ seem to be less influential than one would infer from the experimental observations. The strong dependency on R_0 can be explained by drift deceleration due to resistive currents inside and outside the plasmoid; the dependency on a_0 can only be that strong if the deceleration caused by currents outside the plasmoid dominates the drift process.

4. ITER Predictions

A comparison for 5mm-sized pellets injected from the high and low field side (HFS / LFS) at 300 and 500 m/s into an ITER ohmic L-mode reference scenario [11] target plasma are plotted in Fig.3-4. Caused by the very small penetration after ablation and the particle drift towards the LFS, the pellet velocity for LFS injections would need to be unrealistically high to match the pellet penetration after deposition in the HFS cases, which seems to be in the order of a few decimetres. The same drift quantity can be obtained by use of the scaling law (which is not fitted to typical ITER configurations), but still, the associated uncertainty for the prediction of the absolute drift displacement is considerable and further validation efforts must be undertaken.

5. Conclusions

Even though the benchmark results must be treated with care because of the high relative measurement error, the observed trends in the experimental results appear to be reproducible. Nevertheless, the simulation results must be considered as preliminary, until better validation data becomes available. The main scaling behaviour of the pellet particle drift could be described by a parameter function, which might be useful for the calculation of more realistic approximations of the pellet source profile within a minimum amount of computing time. Due to the high ablation rate in ITER, the pellet simulations seem to indicate that sufficient pellet particle penetration can only be reached by exploitation of the ∇B-drift, if the pellet is injected from the high field side, however, with respect to the high uncertainties of the code validation mentioned above, a final conclusion cannot yet be drawn.

Acknowledgements

This work has been conducted under the European Fusion Development Agreement and performed within EURATOM/ÖAW-Association. The content of the publication is in the responsibility of the authors and does not necessarily represent the views of the European Commission and its services.

References

[1] Pégourié B. et al., Plasma Phys. Control. Fusion 47 (2005) 17
[2] Pégourié B. et al., Nucl. Fusion 47 (2007) 44-56
[3] Terranova D. et al., Nucl. Fusion 47 (2007) 288-296
[4] Pégourié B. et al., EPS 2007, P4.092
[5] Jernigan T.C. et al., APS/DPP 2000, GP1.122
[6] Jones T.T.C. et al., Descriptive Analysis of 1999 Task Force P Data, EURATOM/UKAEA, 1-16
[7] Nehme H., PhD thesis, University of Marseille, to be submitted this year.
[8] Parks P.B., Sessions W.D. and Baylor L.R., Phys. Plasmas (2000) 7 1968-1975
[9] Rozhansky V. et al., Plasma Phys. Control. Fusion 46 (2004) 575-591
[10] Garzotti L. et al., Nucl. Fusion 43 (2003) 1829-1836
[11] ITER Physics Basis, Nucl. Fusion 38 (1999) 2137
[12] Köchl F. et al., EPS 2007, P1.143

Tokamak scenario	Measured drift estimate	Calculated drift
FTU LFS	~3 ± 2 cm	4,2 cm ± 9.3% ± 0.6%
Tore Supra LFS	0–12 cm	12,9 cm ± 5.7% ± 3.1%
Tore Supra HFS	0–8 cm	8,9 cm ± 5.7% ± 3.1%
DIII-D HFS (#99477)	~20 cm	10,2 cm ± 5.5% ± 4.0%
JET LFS (#49223)	~10 ± 6 cm	11,0 cm ± 3.7% ± 4.1%

Table 1 – Comparison of the measured average drift displacement, determined by evaluation of the barycentres of the ablation and deposition profiles, using the same kind of measurement data and calculation methods as in [12], with simulation results for typical tokamak scenarios in terms of minor radius flux coordinate. The indicated measurement error or measurement range refers to the analysis and values indicated in [3-6,12]. The error for the simulation results scales with the measurement error and is very sensitive to the correct determination of the net pellet mass and injection velocity. Relative simulation error estimates are given for a supposed measurement error of Δr_p = 0.2mm and ΔV_p = 50m/s resp..

	C_1	C_2	C_3	C_4	C_5	C_6	C_7	C_8	C_9	C_{10}	C_{11}	C_{12}	C_{13}	σ	$\sigma_{rel.}$
Δ_1	0.116	0.120	0.368	0.041	0.015	1.665	0.439	0.217	-0.038	0.493	0.193	-0.346	-0.204	0.031m	28.0%
Δ_2	0.064	0.192	0.105	0.025	0.077	1.500	0.899	0.955	0.031	0.671	0.377	-0.493	-0.026	0.032m	29.2%
λ_{abl}	0.726	-0.078	-0.174	0.036	0.161	0.133	0.030	0.854	-0.039	0.103	-0.001	-0.051	0.022	0.035	4.5%
λ_{dep}	0.488	-0.056	-0.137	0.031	0.133	0.131	0.330	2.327	0.028	0.082	-0.001	-0.037	0.024	0.047	5.9%

Table 2 – Scaling law constants $C_{1\text{-}13}$, standard deviation σ and relative error $\sigma_{rel.}$ for the calculation of the average drift displacement in terms of minor radius flux coordinates, putting more statistical weight on available pellet injection and typical target plasma configurations at European tokamaks such as FTU, TS, and JET (Δ_1) and using equi-distributed parameter configurations for arbitrary tokamak geometries (Δ_2; a_0<1.4m, R_0<4m). Constants are also listed for the calculation of the ablation and deposition profile barycentres (λ_{abl} and λ_{dep}) in terms of normalised minor radius flux coordinates, using the same parameter scaling formula as given in section 3. Important parameter dependencies are highlighted.

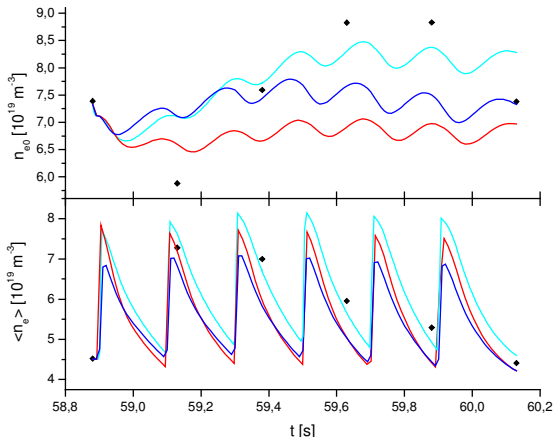

Figure 1 – Axial (top) and average (bottom) density time traces for JETTO simulations of JET experiment #49030, using the mixed Bohm/gyroBohm transport model [10]; red colour: NGPS, cyan colour: pellet code without pre-cooling, blue colour: pellet code with pre-cooling; black diamonds correspond to LIDAR measurements.

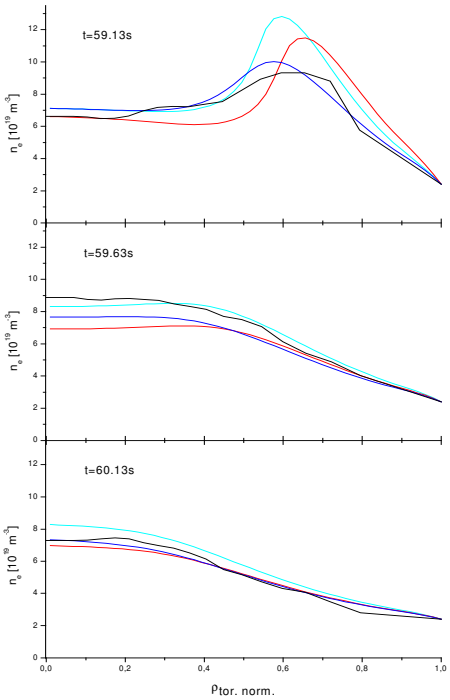

Figure 2 (right) – Comparison of density profile evolution for JETTO simulations of JET experiment #49030; the colour code is the same as in Fig. 1.; LIDAR measurements are shown in black.

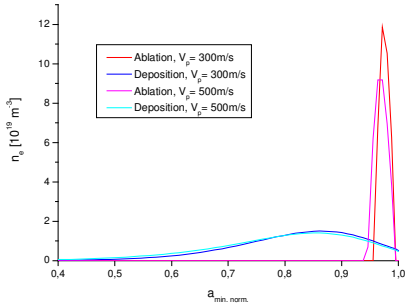

Fig. 3 – ITER HFS pellet injections

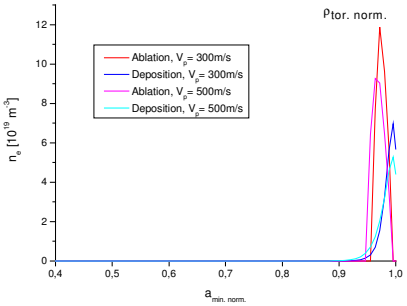

Fig. 4 – ITER LFS pellet injections